Supplemental Material
Spectroscopy along Flerovium Decay Chains: Fine Structure in Odd-A ^{289}Fl

The Supplemental Material provides detailed results and statistical assessments in the analysis of events stemming from decay chains starting with the isotope ^{289}Fl. Table I summarises the information on correlated α-decay chains, which were observed in the present experiment, and which were associated with decays of the even-odd ^{289}Fl.

Decay properties such as decay energies and lifetimes, relating to various ensembles of data associated with previous experiments in the direct or indirect production of ^{289}Fl and with the present experiment (cf. Table I), are compiled: Distributions of decay energies and correlation times along with determined E_α and $T_{1/2}$ values are presented for the different ensembles in Figs. 1 and 2 for ^{289}Fl as well as ^{285}Cn and ^{281}Ds, respectively. To achieve consistency among the TASCA experiments, α-decay energies in Table IV of Ref. [5] were treated with the recoil-correction method outlined in Ref. [1], which led to a reduction of 20-25 keV of the tabulated values. An overview, together with a statistical assessment of the correlation times attributed to the single decay steps is presented Table II for the ensembles of decay chains corresponding to Figs. 1 and 2.

Figure 3 shows an overview of energy-energy, energy-time, and time-time correlations along the ^{289}Fl decay chains. Data is presented in subsets (different colors) relevant for the discussion in the main article. Table III provides the corresponding statistical measures, and Table IV lists corresponding α-hindrance factors [14].

[1] A. Såmark-Roth *et al.*, submitted to Phys. Rev. C.
[2] Yu.Ts. Oganessian *et al.*, Phys. Rev. C **62**, 041604(R) (2000).
[3] Yu.Ts. Oganessian *et al.*, Phys. Rev. C **69**, 054607 (2004).
[4] Ch.E. Düllmann *et al.*, Phys. Rev. Lett. **104**, 252701 (2010).
[5] J.M. Gates *et al.*, Phys. Rev. C **83**, 054618 (2011).
[6] A. Yakushev *et al.*, Inorg. Chem. **53**, 1624 (2014).
[7] A. Yakushev *et al.*, Front. Chem. **10**, 976635 (2022).
[8] Yu.Ts. Oganessian *et al.*, Phys. Rev. C **63**, 011301(R) (2000).
[9] Yu.Ts. Oganessian *et al.*, Phys. Atom. Nucl. **64**, 1349 (2001).
[10] Yu.Ts. Oganessian *et al.*, JINR preprint, E7-2004-160, pp. 1–28 (2004).
[11] S. Hofmann *et al.*, Eur. Phys. J. A **48**, 62 (2012).
[12] D. Kaji *et al.*, J. Phys. Soc. Jpn. **86**, 034201 (2017).
[13] K.-H. Schmidt, Eur. Phys. J. A **8**, 141 (2000).
[14] C. Qi, F.R. Xu, R.J. Liotta, R. Wyss, M.Y. Zhang, C. Asawatangtrakuldee, and D. Hu, Phys. Rev. C **80**, 044326 (2009).

TABLE I: Information on observed correlated α-decay chains suggested to stem from the odd-A flerovium isotope ^{289}Fl. Mid-target beam energies in the laboratory frame, $\langle E_{\rm lab}\rangle$, and the center-of-mass frame, $\langle E_{\rm com}\rangle$, as well as target isotope are provided. Energies of the implanted recoils, $E_{\rm rec}$, the implantation detector strip numbers in x and y, and the assigned isotope of chain origin are listed for each chain. For each decay step, i, the decay energy, E_i, correlation time, Δt_i, and, if in prompt coincidence, photon energies, $E_{\rm ph}$, and electron energies, E_{e^-}, are given. In case of a spontaneous fission (SF) event, the number of prompt hits in the Ge-detector crystals, $N_{\rm Ge}$, is provided instead of any specific photon energy. $N_{\rm random}$ indicates the number of chains of a given type expected to arise from random background. Entries in bold were recorded during beam-off periods. Entries in italic relate to tentative or insecure assignments, typically in connection with a missing event in a chain. Uncertainties of individual energy measurements are $\leq$ 10 keV at typical α-decay energies of 9-10 MeV in the implantation detector. This uncertainty is worse, $\approx$ 20 keV, for reconstructed events because of the energy straggling in the deadlayers of the Si detectors. See Ref. [1] for more details.

No.	$\langle E_{\rm lab}\rangle$ (MeV) $\langle E_{\rm com}\rangle$ (MeV) target[a]	$E_{\rm rec}$ (MeV) pixel (x,y) isotope	E_1 (MeV) Δt_1 (s) E_{ph} (keV) E_{e^-} (MeV)	E_2 (MeV) Δt_2 (s) E_{ph} (keV) E_{e^-} (MeV)	E_3 (MeV) Δt_3 (s) E_{ph} (keV) E_{e^-} (MeV)	E_{SF} (MeV) Δt_{SF} (s) $N_{\rm Ge}$	$N_{\rm random}$
15	237 36.5 ^{244}Pu[a]	13.0 (24/23,20)[b] ^{289}Fl	missing - - -	**9.18(1)** ***120.397*** [c] -		**226** **7.000** **4**	0.04
16	237 36.5 ^{244}Pu[a]	12.0 (26,16) ^{289}Fl	**9.82(1)**[d] **8.680** - -	**9.13(2)**[e] **55.448** **124(1)** -		**219+2** **14.035** **8**	7×10^{-7}
17	237 36.5 ^{244}Pu	19.5 (25,12) ^{289}Fl	**9.99(2)**[e] **0.448** - -	**9.30(2)**[e] **27.535** - -		194 49.835	4×10^{-5}
18	237 36.5 ^{244}Pu	12.8 (13,13) ^{289}Fl	**9.80(1)**[f] **1.945** [c] -	**9.14(1)** **122.202** [c] -		**198+8** **50.949** **7**	7×10^{-7}
19	237 36.5 ^{244}Pu	14.6 (11,17) ^{289}Fl	**9.79(1)**[f] **8.635** [c] -	**9.14(2)**[e] **16.510** [c] -		**199+10**[g] **53.231** **8**	7×10^{-7}
20	237 36.5 ^{244}Pu	missing[h] (11,15) ^{289}Fl	**9.80(1)** - [c] -	**9.16(1)** **50.256** [c] -		**242** **11.943** **11**	3×10^{-5}
21	237 36.5 ^{244}Pu	missing[h] (31,16) ^{289}Fl	**9.81(1)** - - -	**9.10(2)**[e] **18.129** - -		**202** **11.450** **9**	3×10^{-5}
22	241 39.2 ^{244}Pu[a]	13.4[i] (7,13) ^{289}Fl	**9.56(1)**[d] ***0.331*** - -	**0.46(1)**[j] **47.595** - -		**199** **10.027** **9**	2×10^{-4}
23	241 39.2 ^{244}Pu[a]	16.5 (21,14) ^{289}Fl	**9.82(1)**[d] **0.914** - -	**9.12(2)**[e] **276.636** [c] -		**202+9** **15.593** **3**	7×10^{-7}

TABLE I: Continued.

No.	$\langle E_{\rm lab}\rangle$ (MeV) $\langle E_{\rm com}\rangle$ (MeV) target[a]	$E_{\rm rec}$ (MeV) pixel (x,y) isotope	E_1 (MeV) Δt_1 (s) E_{ph} (keV) $E_{e\text{-}}$ (MeV)	E_2 (MeV) Δt_2 (s) E_{ph} (keV) $E_{e\text{-}}$ (MeV)	E_3 (MeV) Δt_3 (s) E_{ph} (keV) $E_{e\text{-}}$ (MeV)	E_{SF} (MeV) Δt_{SF} (s) $N_{\rm Ge}$	$N_{\rm random}$
24	241 39.2 ^{244}Pu	11.3 (5,15) ^{289}Fl	missing - - -	**9.1($\frac{6}{2}$)**[k] ***23.049*** - -		**123+17** **12.359** **4**	0.04
25	241 39.2 ^{244}Pu	15.5 (23,13) ^{289}Fl	9.83(1) 2.223 - -	**9.18(1)** **117.641** [c] -		**183+13** **4.504** **9**	1×10^{-4}
26	241 39.2 ^{244}Pu	14.8 (10,13) ^{289}Fl	**9.79(2)**[ef] **6.007** **339(1)** -	**3.33(1)**[j] **84.973** **142(2)** **0.14(1)**[l]		**197+4** **7.596** **4**	2×10^{-4}
27	241 39.2 ^{244}Pu	15.8 (25,13) ^{289}Fl	**9.91(2)**[ef] **1.455** - -	**8.92(1)**[m] **45.992** - **0.25(1)**[l]		**224** **6.651** **8**	7×10^{-7}
28	241 39.2 ^{244}Pu	14.0 (21,18) ^{289}Fl	**9.79(1)**[f] **1.296** [c] -	**0.36(1)**[j] **26.815** - -	**8.63(1)** **251.807**[n] - -	**240** **0.00136** **5**	2×10^{-8}
29	237 36.5 ^{244}Pu	13.3 (16,4) ^{289}Fl	missing[o] - - -	9.09(1) *145.521* - -	**8.68(1)** **21.834** [p] -	**188** **0.0736** **4**	9×10^{-9}

[a]For the first part of the experiment, the target wheel comprised one segment of enriched ^{242}Pu and three segments of enriched ^{244}Pu. For the second part of the experiment, all four segments of the target wheel were made of enriched ^{244}Pu. See Ref. [1] for details.

[b]The energy split, $\approx 50:50$, between the n-side strips is consistent for all events reported for this chain.

[c]Delayed γ ray(s) observed within $\Delta t = [1,7]$ µs.

[d]Event triggered 200-s beam shutoff.

[e]Reconstructed event (cf. Ref. [1]). Detected energies in the implantation detector and in the box DSSSD were: chain 16: 1.41(1) and 6.57(1) MeV; chain 17: 0.58(1) and 8.88(1) MeV as well as 0.74(1) and 7.97(1) MeV; chain 19: 0.64(1) and 7.92(1) MeV; chain 21: 0.62(1) and 7.90(1) MeV; chain 23: 0.59(1) and 7.76(1) MeV; chain 26: 0.73(1) and 8.50(1) MeV; chain 27: 0.95(1) and 8.15(1) MeV.

[f]Event triggered 300-s beam shutoff.

[g]A 5.65(1)-MeV escape-like event was registered 17.983 s prior to the fission event. See Ref. [1] for details.

[h]Implantation event searched for in a period of 60 s prior to the first α-decay event in the chain.

[i]Another 14.5-MeV implant candidate event 0.580 s earlier.

[j]Escape event. See Ref. [1] for details.

[k]Unable to determine pixel within the box DSSD due to all n-strips within box detector firing. Reconstructed energies assuming the hit was in n-strip 0 and 15 results in 9.7 and 8.9 MeV, respectively. The given value is the solid-angle weighted mean.

[l]About 13% of the full-energy α-events in the energy interval [8.5,10.5] MeV come in prompt coincidence with an electron. See Ref. [1] for details.

[m]The probability to observe an α-decay event within [8.5,9.5] MeV within the time period of the entire decay chain (54.1 s) is 7×10^{-4}. A 0.60(1)-MeV escape-like event was registered 30.237 s earlier. See Ref. [1] for details.

[n]750-s period used for $N_{\rm random}$ instead of the 110-s period as discussed in Ref. [1].

[o]No viable candidate within 20 s after the implantation event.

[p]Event close to the beam-on period with many Ge crystals signaling.

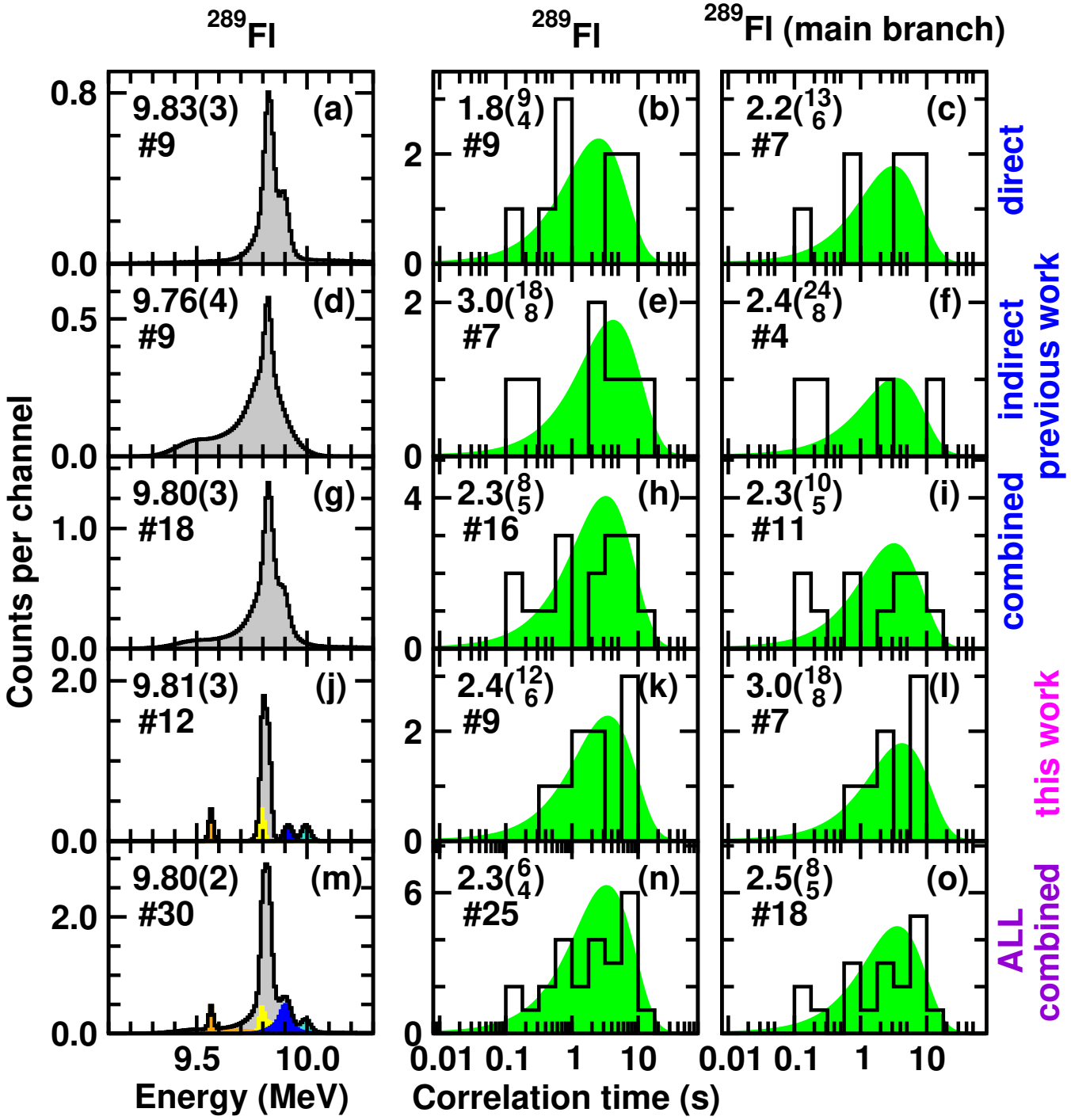

FIG. 1: (Color online) The left column provides experimental decay-energy spectra from events associated with the decay step $^{289}\mathrm{Fl} \rightarrow {}^{285}\mathrm{Cn}$. For a single entry, a Gaussian with integral one and a width compliant with its measured uncertainty was added into the respective spectrum. The numbers at the top left of each panel in the left column are the (α-decay) energies extracted by computing the histogram mean in the interval [9.4,10.2] MeV. The middle column provides the correlation-time analysis for *all* decays associated with ^{289}Fl, while the right column selects only those events associated with the *main branch* ($E_\alpha \approx 9.81$ MeV) of ^{289}Fl. Experimental data points are comprised in the histograms (black lines). The shaded areas (green) provide correlation-time distributions expected for the corresponding half lives, $T_{1/2}$, which are given in the top left corner of each panel. For all panels, the number after the hashtag, #, indicates the number of available data points. The first row, panels (a)-(c), refers to previous direct production of ^{289}Fl [2–7]. The second row, panels (d)-(f), refers to previous indirect production of ^{289}Fl [8–12]. The spectra in the third row, panels (g)-(i), are the sums of the spectra in the first and second row. The fourth row, panels (j)-(l), refers to the present data (cf. Table I). The spectra in the fifth row, panels (m)-(o), are the sums of the spectra in the third and fourth row, i.e., comprise current best values for the (main) decay characteristics of ^{285}Cn. Orange (blue) color in panels (j) and (m) indicates suggested low-energy (high-energy) decay branches in ^{289}Fl (see main article). Yellow color refers to chains reaching a Hs isotope. The single chain No. 17 in Table I is marked cyan.

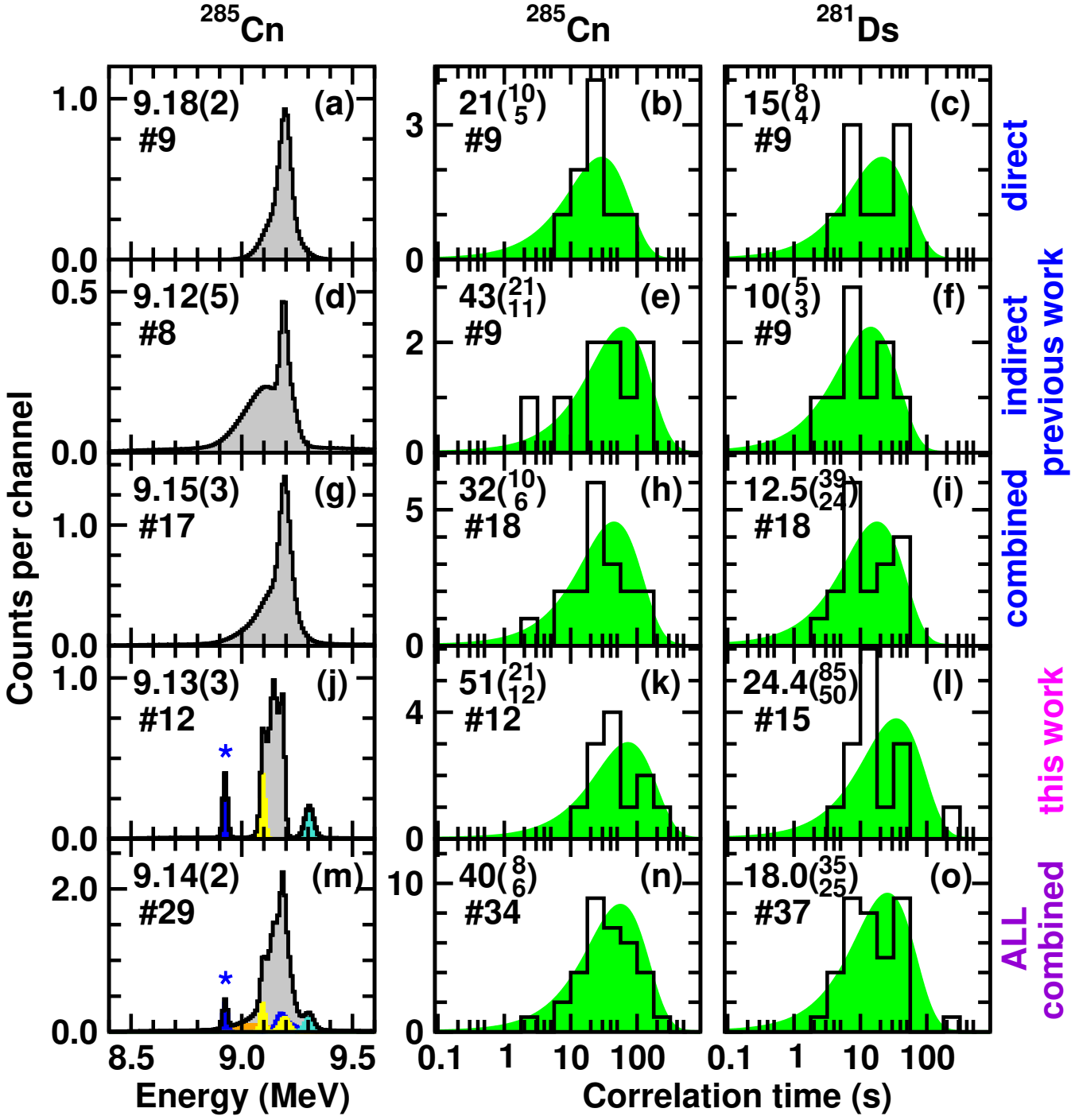

FIG. 2: (Color online) The left column provides experimental decay-energy spectra from events associated with the decay step ^{285}Cn $\rightarrow$ ^{281}Ds. For a single entry, a Gaussian with integral one and a width compliant with its measured uncertainty was added into the respective spectrum. The numbers at the top left of each panel in the left column are the (α-decay) energies extracted by computing the histogram mean in the interval [8.6,9.6] MeV. The middle and right columns provide the correlation-time analysis for *all* decays associated with ^{285}Cn and ^{281}Ds, respectively. Experimental data points are comprised in the histograms (black lines). The shaded areas (green) provide correlation-time distributions expected for the corresponding half lives, $T_{1/2}$, which are given in the top left corner of each panel. For all panels, the number after the hashtag, #, indicates the number of available data points. The first row, panels (a)-(c), refers to previous direct production of ^{289}Fl [2–7] The second row, panels (d)-(f), refers to previous indirect production of ^{289}Fl [8–12]. The spectra in the third row, panels (g)-(i), are the sums of the spectra in the first and second row. The fourth row, panels (j)-(l), refer to the present data (cf. Table I). The spectra in the fifth row, panels (m)-(o), are the sums of the spectra in the third and fourth row, i.e., comprise current best values for the (main) decay characteristics of ^{289}Fl. Orange (blue) color in panels (j) and (m) indicates suggested low-energy (high-energy) decay branches in ^{289}Fl (see main article). Note that the 8.92(1)-MeV α event ($\star$), was detected in prompt coincidence with a 0.25(1)-MeV electron. Yellow color refers to chains reaching a Hs isotope. The single chain No. 17 in Table I is marked cyan.

TABLE II: Overview of correlation time analyses of single decay steps according to Ref. [13] of various ensembles of decay chains associated with previous direct and indirect and present direct production of ^{289}Fl. These are the same ensembles as displayed in the corresponding rows of Figs. 1 and 2.

Label	previous direct	previous indirect	previous combined	this work	all combined
No. of chains	9	9	18	15	33
References	[2–7]	[8–12]			
$T_{1/2}(^{289}\mathrm{Fl})$ (s)	$1.8(^{9}_{4})$	$3.0(^{18}_{8})$	$2.3(^{8}_{5})$	$2.4(^{12}_{6})$	$2.3(^{6}_{4})$
data points; $\sigma_{\Theta,\mathrm{exp}}$	9 ; 1.32	7 ; 1.58	16 ; 1.45	9 ; 0.97	25 ; 1.31
$[\sigma_{\Theta,\mathrm{low}}, \sigma_{\Theta,\mathrm{high}}]$ [13]	[0.62,1.84]	[0.52,1.87]	[0.77,1.75]	[0.62,1.84]	[0.85,1.71]
data points; E_{decay} (MeV)[a]	9 ; 9.83(3)	9; 9.76(4)	18; 9.80(3)	12 ; 9.81(3)	30 ; 9.80(2)
$T_{1/2}(^{285}\mathrm{Cn})$ (s)	$21(^{10}_{5})$	$43(^{21}_{11})$	$32(^{10}_{6})$	$51(^{21}_{12})$	$40(^{8}_{6})$
data points; $\sigma_{\Theta\,\mathrm{exp}}$	9 ; 0.69	9 ; 1.29	18 ; 1.06	12 ; 0.80	34[c] ; 0.99
$[\sigma_{\Theta,\mathrm{low}}, \sigma_{\Theta,\mathrm{high}}]$ [13]	[0.62,1.84]	[0.62,1.84]	[0.79,1.73]	[0.70,1.79]	[0.91,1.65]
data points; E_{decay} (MeV)[b]	9 ; 9.18(2)	8; 9.12(5)	17; 9.15(3)	12 ; 9.13(3)	29 ; 9.14(2)
$T_{1/2}(^{281}\mathrm{Ds})$ (s)	$15(^{8}_{4})$	$10(^{5}_{3})$	$12.5(^{39}_{24})$	$24.4(^{85}_{50})$	$18.0(^{35}_{25})$
data points; $\sigma_{\Theta,\mathrm{exp}}$	9 ; 0.84	9 ; 0.85	18 ; 0.87	15 ; 1.03	37[c] ; 0.97
$[\sigma_{\Theta,\mathrm{low}}, \sigma_{\Theta,\mathrm{high}}]$ [13]	[0.62,1.84]	[0.62,1.84]	[0.79,1.73]	[0.75,1.76]	[0.93,1.63]
data points; E_{decay} (MeV)[d]	1 ; 8.71(2)	–	1 ; 8.71(2)	2 ; 8.66(2)	3 ; 8.67(2)
$T_{1/2}(^{277}\mathrm{Hs})$ (ms)	$3.1(^{149}_{14})$	–	$3.1(^{149}_{14})$	$26(^{64}_{11})$	$18(^{25}_{7})$
data points; $\sigma_{\Theta,\mathrm{exp}}$	1	–	1	2	3 ; 1.67
$[\sigma_{\Theta,\mathrm{low}}, \sigma_{\Theta,\mathrm{high}}]$ [13]	–	–	–	–	[0.19,1.91]

[a]Result from the integration of the energy spectra in the left column of Fig. 1 in the interval [9.2,10.2] MeV.
[b]Result from the integration of the energy spectra in the left column of Fig. 2 in the interval [8.6,9.6] MeV.
[c]Half-life analyses of ^{285}Cn and ^{281}Ds include four decay chains from Fl-chemistry experiments behind TASCA [6, 7].
[d]Result from the integration of the energy spectra in the interval [8.4,9.0] MeV.

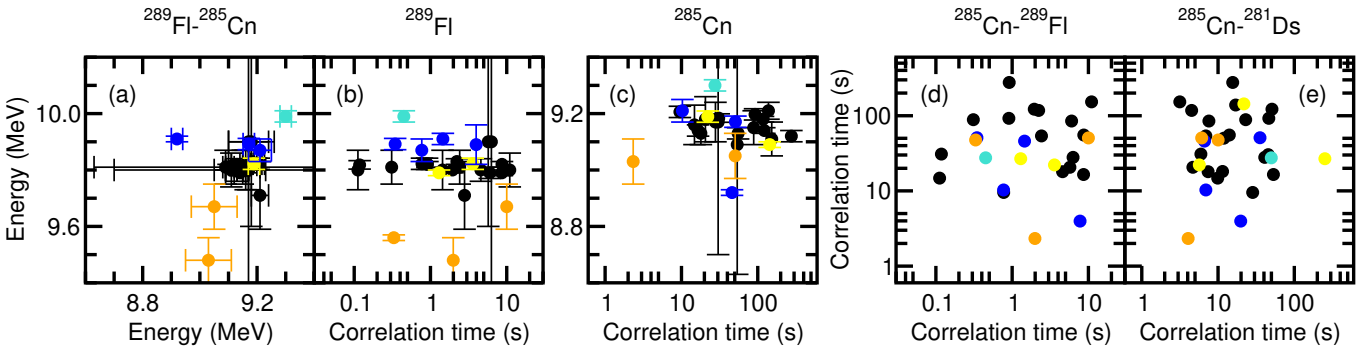

FIG. 3: Energy-energy correlations between α-decay events of ^{289}Fl and ^{285}Cn are displayed in (a). Energy-time correlations are shown in (b) and (c) for ^{289}Fl and ^{285}Cn events, respectively. Note that panels (a) and (b) are identical to Fig. 2(a) and (b) of the main article. Time-time correlations are plotted in (d) and (e) for ^{289}Fl-^{285}Cn and ^{285}Cn-^{281}Ds combinations, respectively. Black circles mark events associated with the main (M) decay branch of ^{289}Fl. Orange and blue circles mark events with low-energy (L) and high-energy (H) α-decay events assigned to ^{289}Fl; see panel (a), the decay sequences in Fig. 3 of the main article, and Table III for details. Yellow circles mark events from the three decay chains ending in ^{277}Hs. The single chain No. 17 in Table I is marked cyan.

TABLE III: Overview of correlation time analyses of single decay steps according to Ref. [13] of various ensembles of decay chains associated with direct and indirect production of ^{289}Fl. These are subsets of the rightmost column labelled 'all combined' in Table II. The label 'low-energy' (set L) refers to chains with $E_\alpha < 9.7$ MeV for ^{289}Fl; one in Ref. [10], one in Ref. [12], and chain No. 22 in Table I [colored orange in Figs. 1(m) and 2(m)]. The label 'high-energy' (set H) refers to chains with full or firmly reconstructed energies with $E_\alpha > 9.85$ MeV; one in Ref. [2, 3], one in Ref. [4, 5], one in Ref. [12], as well as chain No. 27 in Table I [colored blue in panels (j) and (m) in Figs. 1 and 2]. Chain No. 17 cannot be accomplished for in this context (cf. Fig. 3 and associated discussion in main article) and remains lonesome. The label 'Hs-chains' refers to the three chains with an α-decay branch into ^{277}Hs, one in Ref. [4, 5] and chains No. 28 and 29 in Table I [colored yellow in Figs. 1(m), 2(m), and Fig. 3].

Label	'low-energy' set L ●	'high-energy' set H ●	● & ● sets H&M	'main branch' set M ●	'Hs-chains' ●
No. of chains	3	4	29	25	3
$T_{1/2}(^{289}\mathrm{Fl})$ (s)	$2.9(^{39}_{10})$	$1.1(^{11}_{4})$		$2.5(^{8}_{5})$	$1.8(^{44}_{8})$
data points; $\sigma_{\Theta,\mathrm{exp}}$	3[a] ; 1.39	4 ; 0.89		18 ; 1.37	2 ; 0.51
$[\sigma_{\Theta,\mathrm{low}}, \sigma_{\Theta,\mathrm{high}}]$ [13]	[0.19,1.91]	[0.31,1.92]		[0.79,1.73]	[0.04,1.83]
data points; E_{decay} (MeV)[b]	3 ; 9.57(6)	4; 9.89(2)		22; 9.80(4)	2 ; 9.81(2)
$T_{1/2}(^{285}\mathrm{Cn})$ (s)	$25(^{34}_{9})$	$21(^{21}_{7})$	$42(^{10}_{7})$	$46(^{13}_{8})$	$45(^{61}_{16})$
data points; $\sigma_{\Theta\,\mathrm{exp}}$	3 ; 1.44	4 ; 0.85	26 ; 0.93	22 ; 0.90	3[c] ; 1.44
$[\sigma_{\Theta,\mathrm{low}}, \sigma_{\Theta,\mathrm{high}}]$ [13]	[0.19,1.91]	[0.31,1.92]	[0.86,1.70]	[0.82,1.74]	[0.19,1.91]
data points; E_{decay} (MeV)[d]	2 ; 9.04(6)	3; 9.10(8)	26 ; 9.14(2)	23; 9.15(2)	2 ; 9.14(4)
$T_{1/2}(^{281}\mathrm{Ds})$ (s)	$5.0(^{68}_{18})$	$14(^{14}_{5})$	$19(^{4}_{3})$	$20(^{5}_{3})$	$65(^{88}_{24})$
data points; $\sigma_{\Theta,\mathrm{exp}}$	3 ; 0.37	4 ; 0.60	29 ; 0.95	25 ; 1.00	3 ; 1.57
$[\sigma_{\Theta,\mathrm{low}}, \sigma_{\Theta,\mathrm{high}}]$ [13]	[0.19,1.91]	[0.41,1.90]	[0.88,1.68]	[0.85,1.71]	[0.19,1.91]
data points; E_{decay} (MeV)[e]	–	–	3 ; 8.67(2)	3 ; 8.67(2)	3 ; 8.67(2)
$T_{1/2}(^{277}\mathrm{Hs})$ (s)	–	–	$0.018(^{25}_{7})$	$0.018(^{25}_{7})$	$0.018(^{25}_{7})$
data points; $\sigma_{\Theta,\mathrm{exp}}$	–	–	3 ; 1.67	3 ; 1.67	3 ; 1.67
$[\sigma_{\Theta,\mathrm{low}}, \sigma_{\Theta,\mathrm{high}}]$ [13]	–	–	[0.19,1.91]	[0.19,1.91]	[0.19,1.91]

[a] Using $\Delta t = 0.331$ s for chain No. 22.
[b] Result from the integration of the energy spectra in the left column of Fig. 1 in the interval [9.2,10.2] MeV.
[c] Using $\Delta t = (145.5 - 1.8)\,\mathrm{s} = 143.7$ s as data point from chain No. 29.
[d] Result from the integration of the energy spectra in the left column of Fig. 2 in the interval [8.6,9.6] MeV.
[e] Result from the integration of the energy spectra in the interval [8.4,9.0] MeV.

TABLE IV: Hindrance factors (HF) according to Ref. [14] for different decay paths considered for ^{289}Fl, ^{285}Cn, and ^{281}Ds. The color code of the filled circles is the same as introduced and used in Figs. 1-3 and Table III.

Isotope	Set	E_x (MeV)	E_α (MeV)	Q_α (MeV)	$T_{1/2}$ (s)	No. chains	br_α (%)	HF
^{2xx}Fl	L	X_1	9.57(3)[a]	9.70(3)	$2.9(^{39}_{10})$	3	100	$0.64(^{97}_{25})$
^{28x}Cn	●	X_2	9.04(6)	9.17(6)	$25(^{34}_{9})$	3	100	$0.56(^{154}_{34})$
^{289}Fl	L&M	0.00	9.57(3)[a]	9.70(3)	$2.6(^{7}_{4})$	3	11	$5.3(^{19}_{13})$
	●&●		9.80(2)[b]	9.94(2)		25	89	$3.3(^{12}_{8})$
^{289}Fl	M	0.00	9.80(2)[b]	9.94(2)	$2.5(^{8}_{5})$	25	100	$2.8(^{12}_{7})$
			8.93(3)[c]	9.06(3)		1	4	$12(^{7}_{4})$
^{285}Cn	●	0.00	9.07(2)[b]	9.20(2)	$46(^{13}_{8})$	17	68	$1.9(^{9}_{5})$
			9.19(2)[b]	9.32(2)		7[d]	28	$11(^{6}_{3})$
^{281}Ds		0.00	8.63(2)[b]	8.75(2)	$20(^{5}_{3})$	3	12	$0.8(^{3}_{2})$
^{289}Fl	M&H	0.07	9.90(3)[b]	10.04(3)	$1.1(^{11}_{4})$	4	100	$2.4(^{31}_{9})$
			8.93(3)[c]	9.06(3)		2	7	$6.1(^{34}_{20})$
^{285}Cn	●&●	0.00	9.07(2)[b]	9.20(2)	$42(^{10}_{7})$	18	62	$2.0(^{8}_{5})$
			9.19(2)[b]	9.32(2)		9[d]	31	$9.3(^{40}_{26})$
^{281}Ds		0.00	8.63(2)[b]	8.75(2)	$19(^{4}_{3})$	3	10	$0.9(^{3}_{2})$
^{2xx}Fl	chain 17	Y_1	9.99(4)[e]	10.13(4)	$0.31(^{148}_{14})$	1	100	$1.2(^{68}_{6})$
^{28x}Cn	●	Y_2	9.30(4)[e]	9.43(4)	$19(^{91}_{8})$	1	100	$2.9(^{162}_{14})$

[a]Uncertainty based on the detected energy of chain No. 22 and full-widths at half-maximum for α-decay lines of the present experiment.

[b]Uncertainty and energy based on peak structure and GEANT4 simulations. A systematic uncertainty of 10 keV was added due to extrapolations of atomic relaxation processes.

[c]Energy and uncertainty based on chains No. 26 and 27 and GEANT4 simulations. A systematic uncertainty of 10 keV was added due to extrapolations of atomic relaxation processes.

[c]Chains 15 and 25 of the present data set plus those with reported $E_\alpha > 9.18$ MeV from previous studies.

[e]Uncertainty based on detected energies along chain No. 17 and full-widths at half-maximum for α-decay lines of the present experiment.